Supplementary for

A novel method for *in-situ* visualization of the growth kinetics, structures and behaviors of gas-phase fabricated metallic alloy nanoparticles

Lei Zhang [a†], Long-Bing He [a, b†*], Lei Shi [a], Yu-Feng Yang [a], Guan-Lei Shang [a], Hua Hong [a] and Li-Tao Sun [a, b*]

a. SEU-FEI Nano-Pico Center, Key Lab of MEMS of Ministry of Education, Southeast University, Nanjing 210096, P. R. China
b. Center for Advanced Materials and Manufacture, Joint Research Institute of Southeast University and Monash University, Suzhou 215123, P

The influence of substrates on the EAD process

Carbon films with different thicknesses (5nm, 15nm, 25nm) are used as supporting substrates to examine the substrate effect. All the micro-balls selected on the supporting films have diameters of around 2 μm and the used e-beam intensity is around 1×10^4 A/m^2. **Figure** S1 shows the results after irradiating the micro-balls on the three different substrates respectively. The micro-ball on the carbon film with thickness of 25 nm retains unchanged, and no nanoparticle is formed in the surrounding area. In contrast, the micro-balls on the carbon films with thicknesses of 5 nm and 15 nm show clear EAD phenomena. Obviously, the EAD phenomenon on the 5-nm-thick carbon film is much more drastic than that on the 15-nm-thick carbon film.

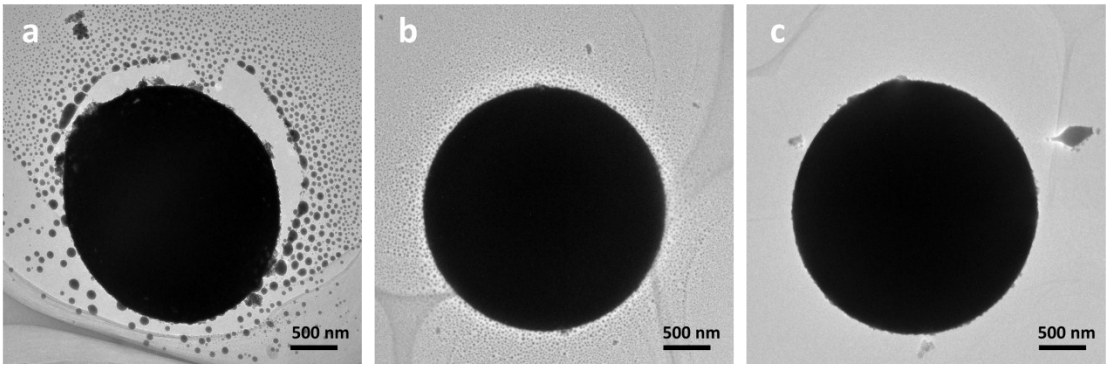

Figure S1. Comparison of the EAD phenomena of micro-balls carbon films with different thicknesses. The thicknesses are **(a)** 5nm, **(b)** 15nm, and **(c)** 25nm.

Scanning thermal microscopy (SThM) is used to characterize the heat conduction effect of the above three substrates. In the SThM, a resistive thermal probe is heated by a sinusoidal current of angular frequency ω and brought into contact with the carbon film substrate. The amplitude of the temperature oscillations of the heat source (sample thickness x) is given as $\Delta T = \frac{P}{\pi k}\left[\frac{1}{2}\ln\left(\frac{2D}{x^2}\right) - 0.5772 - \frac{\mathrm{j}\pi}{x} - \ln(\omega)\right]$, where P is the power dissipated into the sample per unit length, k and D are the sample thermal conductivity and the thermal diffusivity respectively. The electrical resistance of the probe depends on its temperature almost linearly, and can be expressed as

$$R(t) = R_{dc} + \Delta R(t) = R_{dc} + \frac{\mathrm{d}R}{\mathrm{d}T}\Delta T \cdot \frac{1}{2}\left[1 - \cos\left(2\omega t - \theta\right)\right] = R^*_{dc} - \frac{\mathrm{d}R}{\mathrm{d}T}\Delta T \cdot \frac{1}{2}\cos\left(2\omega t - \theta\right),$$

where R^*_{dc} is the mean resistance, θ is the phase shift of ΔT with respect to the power oscillation, and $\mathrm{d}R/\mathrm{d}T$ is the temperature coefficient of the probe. Accordingly, the voltage drop along the probe is the result of the applied current and the electric resistance, i.e. $U(t) = R(t)I(t) = R^*_{dc} I_0 \sin(\omega t) - I_0 \frac{\mathrm{d}R}{\mathrm{d}T}\frac{\Delta T}{2}\sin(\omega t)\cos(2\omega t - \theta)$

$= (R^*_{dc} I_0) \cdot \sin(\omega t) + I_0 \frac{\mathrm{d}R}{\mathrm{d}T} \frac{\Delta T}{4} \sin(\omega t - \theta) - I_0 \frac{\mathrm{d}R}{\mathrm{d}T} \frac{\Delta T}{4} \sin(3\omega t - \theta)$. It shows that the 3ω component is independent of the mean resistance and therefore its amplitude only affects the value of periodic thermal probe temperature. By extracting the 3ω-signal subsection $U_{3\omega}$ from the measured voltage drop and plotting it versus the logarithmic angular frequency ω, the resulted line slop is resulted to be inversely proportional to the thermal conductivity k.

$$\frac{U_{3\omega_1} - U_{3\omega_2}}{\ln(\omega_1) - \ln(\omega_2)} = \frac{I_0}{4} \frac{\mathrm{d}R}{\mathrm{d}T} \frac{P}{\pi k}$$

The test results of the three carbon film substrates are recorded in **Figure S2**. As the power dissipation P is independent of the frequency, a high thermal conductivity can be concluded for the thick carbon film.

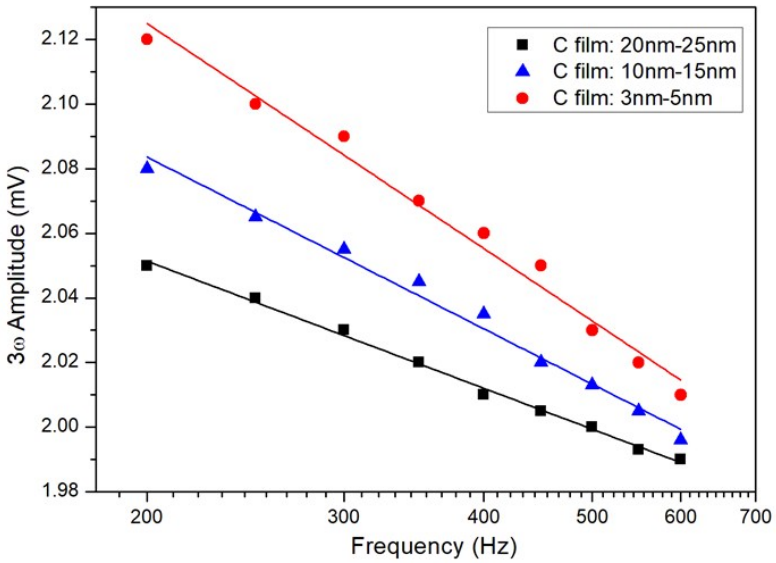

Figure S2. SThM test results of the three carbon film substrates. The thicker the carbon film is, the larger its heat conductivity is.

Nanoparticles oxidation

Figure S3 shows several oxidized nanoparticles after exposure to the atmosphere. Oxide shells can be easily identified. After oxidation, the nanoparticles remain stable without coalescence even though they are almost toughed with each other.

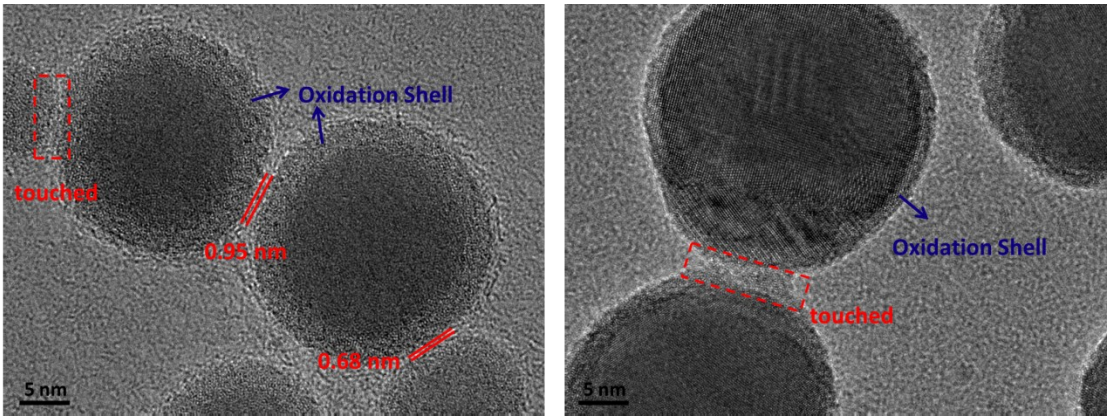

Figure S3. Oxidized nanoparticles after exposure to the atmosphere. The nanoparticles remain stable without coalescence.

Calculation of the saturation vapor pressures of Bi, Pb, Sn and In

The saturation vapor pressure is calculated by the equation developed by Yaws *et al* [1] as $\log P = A + \frac{B}{T} + C\log T + DT + ET^2$, where P is the saturation vapor pressure, T is the thermodynamic temperature, A, B, C, D and E are the fitting constants and their values for Bi, Pb, Sn and In are shown in **Table S1**. **Figure S4** shows the calculated saturation vapor pressures of Bi, Pb, Sn and In in their bulk state. Obviously, the vapor pressures of Bi and Pb are much higher than those of In and Sn.

Table S1. Values of fitting constants in saturation vapor pressure equation

	A	B	C	D	E
Bi	1449.1712	-8.3717×10^{4}	-5.1359×10^{2}	2.0492×10^{-1}	-2.9858×10^{-5}
Pb	-17.6204	-8.5777×10^{3}	9.2106	-3.9318×10^{-3}	5.4789×10^{-7}
In	112.3721	-1.8894×10^{4}	-3.5777×10^{1}	1.1333×10^{-2}	-1.3444×10^{-6}
Sn	-11.8452	-1.3744×10^{4}	6.4004	-9.7861×10^{-4}	-4.2795×10^{-10}

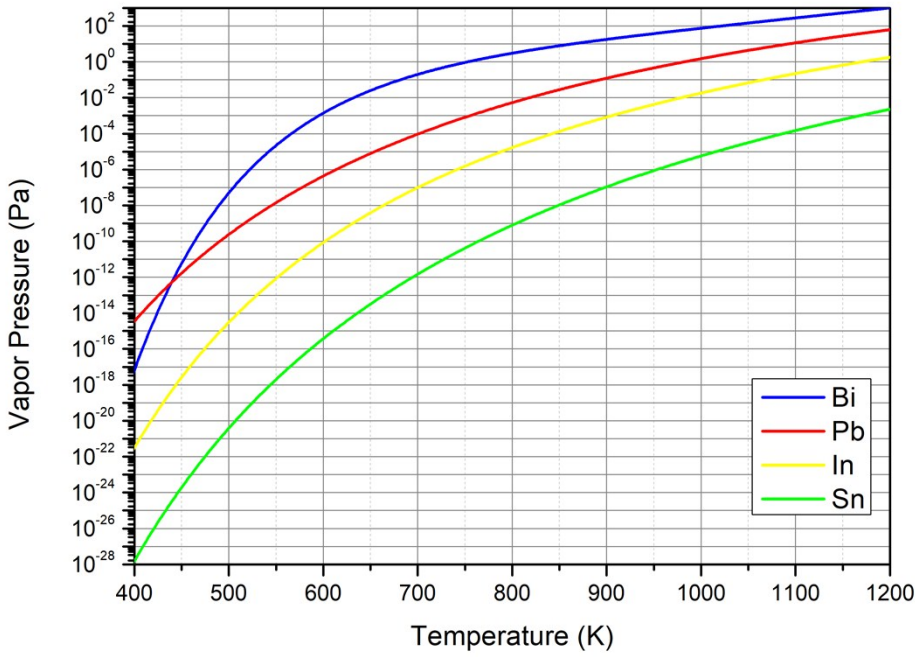

Figure S4. Saturation vapor pressure of Bi, Pb, Sn and In.

Coalescence of nanoparticles

Coalescences involve four (red) and five (blue) nanoparticles respectively are shown in **Figure S5**. It is found that the average inter-particle spacings in these two events are different significantly. The average inter-particle spacing among the nanoparticles marked in red is around 7.4 nm while that for the blue is around 3.1 nm. Interestingly, the inter-particle spacing between nanoparticles 1 and 2 is smaller than

that between nanoparticles 1 and 3. Moreover, there are also nanoparticles keeping isolated without coalescence even though they have a small inter-particle spacing. Hence the inter-particle spacing should not be the only criterion in judging the coalescence events.

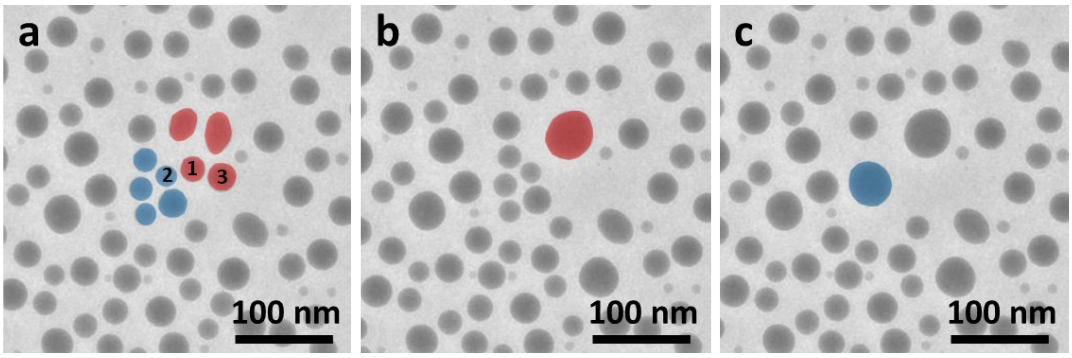

Figure S5. Coalescence events involving four and five nanoparticles, respectively.

Reference

[1] C. L. Yaws, Handbook of vapor pressure: volume 4: inorganic compounds and elements, Gulf Professional Publishing, 1995.